JOC Article

Crystal Engineering for $\pi-\pi$ Stacking via Interaction between Electron-Rich and Electron-Deficient Heteroaromatics

Yu-Chang Chang,[†] Yu-Da Chen,[‡] Chih-Hsin Chen,[†] Yuh-Sheng Wen,[†] Jiann T. Lin,*[,†] Hsing-Yin Chen,[§,†] Ming-Yu Kuo,[||,†] and Ito Chao*[,†]

Department of Chemistry and Biochemistry, National Chung Cheng University, Chia-Yi, 621, Taiwan, Institute of Chemistry, Academia Sinica, 115 Nankang, Taipei, Taiwan

jtlin@chem.sinica.edu.tw; ichao@chem.sinica.edu.tw

Received March 10, 2008

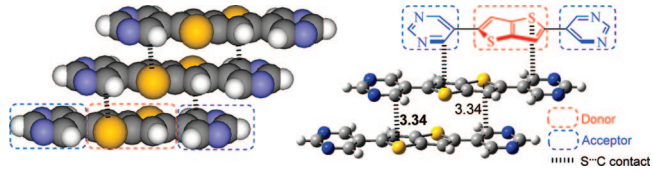

New dipolar compounds containing alternating electron-rich thieno[3,2-*b*]thiophene units and electron deficient units have been synthesized. Compounds with 5-pyrimidinyl (compound **2**) or benzothiazole (compound **5**) as the electron-deficient unit were structurally characterized by the single-crystal X-ray diffraction method. The arrangement of the molecules is found to be one-dimensional slipped-π-stack for **2**. That of **5** is of slipped-π-stack, albeit with a tilt angle between neighboring π-stacks. The $\pi-\pi$ interfacial distances of the molecules in the crystal lattice are 3.47 and 3.59 Å for **2** and **5**, respectively. On the basis of the crystal structure, compound **2,** with negligible $\pi-\pi$ slip along the short axis of the molecules, has a calculated electronic coupling value (0.153 eV) twice as large as that of the largest coupling of pentacene. Accordingly, the theoretically estimated hole mobility (μ^+) for **2** (2.32 $cm^2\ s^{-1}\ V^{-1}$) compares favorably with that of pentacene (1.93−5.43 $cm^2\ s^{-1}\ V^{-1}$), despite of the larger reorganization energy for hole transport in **2**. The symmetric intrastack S···C contacts found between the thieno[3,2-*b*]thiophene and pyrimidinyl units explain the unique features of the crystal structure of **2** and the resulting large electronic coupling.

Introduction

There have been a growing number of efforts in the pursuit of a face-to-face $\pi-\pi$ stacking array in the solid-state packing of organic semiconductors, due to the potentially improved electrical characteristics largely promoted by the good intermolecular $\pi-\pi$ interaction.[1–4] Herringbone packing arrangement of the promising p-type semiconductors such as oligoacenes constricts the realization of their potentially high carrier mobility.[5] Recent studies demonstrate that through structural modification of the commonly employed oligoacenes, for example, the herringbone packing could be forced into a π-stacked manner by destroying their C−H···π interaction between acenes, and may lead to better mobility.[4] Anthony and co-workers successfully showed that functionalizing the bulky alkynyl groups at

[†] Academia Sinica.
[‡] National Chung Cheng University.
[§] Current address: Faculty of Medicinal and Applied Chemistry, Kaohsiung Medical University, Kaohsiung 807, Taiwan,
[||] Current address: Department of Applied Chemistry, National Chi Nan University, Nantou 545, Taiwan

(1) (a) Li, X. C.; Sirringhaus, H.; Garnier, F.; Holmes, A. B.; Moratti, S. C.; Feeder, N.; Clegg, W.; Teat, S. J.; Friend, R. H. *J. Am. Chem. Soc.* **1998**, *120*, 2206. (b) Garnier, F.; Horowitz, G.; Fichou, D.; Yassar, D. *Synth. Met.* **1996**, *81*, 163. (c) Dimitrakopoulos, C. D.; Furman, B. K.; Graham, T.; Hegde, S.; Purushothaman, S. *Synth. Met.* **1998**, *92*, 47. (d) Laquindanum, J. G.; Katz, H. E.; Lovinger, A. J.; Dodabalapur, A. *Adv. Mater.* **1997**, *9*, 36. (e) Sirringhaus, H.; Brown, P. J.; Friend, R. H.; Nielson, M. M.; Bechgaard, K.; Langeveld-Voss, B. M. W.; Spiering, A. J. H.; Janssen, R. A.; Meijer, E. W.; Herwig, P.; de Leeuw, D. M. *Nature* **1999**, *401*, 685.

(2) (a) Ie, Y.; Nitani, M.; Ishikawa, M.; Nakayama, K.-i.; Tada, H.; Kaneda, T.; Aso, Y. *Org. Lett.* **2007**, *9*, 2115. (b) Sokolov, A. N.; Friščić, T.; MacGillivray, L. R. *J. Am. Chem. Soc.* **2007**, *128*, 2806. (c) Payne, M. M.; Odom, S. A.; Parkin, S. R.; Anthony, J. E. *Org. Lett.* **2004**, *6*, 3325. (d) Anthony, J. E. *Angew. Chem., Int. Ed.* **2008**, *47*, 452. (e) Ahmed, E.; Briseno, A. L.; Xia, Y.; Jenekhe, S. A. *J. Am. Chem. Soc.* **2008**, *130*, 1118. (f) Li, L.; Tang, Q.; Li, H.; Yang, X.; Hu, W.; Song, Y.; Shuai, Z.; Xu, W.; Liu, Y.; Zhu, D. *Adv. Mater.* **2007**, *19*, 2613. (g) Janzen, D. E.; Burand, M. W.; Ewbank, P. C.; Pappenfus, T. M.; Higuchi, H.; da Silva Filho, D. A.; Young, V. G.; Brédas, J.-L.; Mann, K. R. *J. Am. Chem. Soc.* **2004**, *126*, 15295. (h) Bader, M. M.; Custelcean, R.; Ward, M. D. *Chem. Mater.* **2003**, *15*, 616. (i) Pappenfus, T. M.; Chesterfield, R. J.; Frisbie, C. D.; Mann, K. R.; Casado, J.; Raff, J. D.; Miller, L. L. *J. Am. Chem. Soc.* **2002**, *124*, 4184. (j) Yassar, A.; Demanze, F.; Jaafari, A.; El Idrissi, M.; Coupry, C. *Adv. Funct. Mater.* **2002**, *12*, 699.

(3) Curtis, M. D.; Cao, J.; Kampf, J. W. *J. Am. Chem. Soc.* **2004**, *126*, 4318. See Results section for more details.

10.1021/jo800546j CCC: $40.75
Published on Web 05/22/2008

the 6,13 positions of pentacene leads to good face-to-face π−π interaction.[4a–d] Kobayashi and co-workers exploited the nonbonded chalcogen−chalcogen interaction[6] to force the 9,10-bis(methylchalcogeno)anthracenes[4e,f] and 6,13-bis(alkylthio)pentacenes[4g] being crystallized into face-to-face π−π stacking in the solid state. Meng, Bao, Wudl, and co-workers reported the hexathiapentacene molecules stacking face-to-face along the *a*-axis facilitated by the intermolecular S···S chalcogen−chalcogen interaction.[4h] For π-stacked 5,11-dichlorotetracene, Bao et al. reported a measured mobility that excelled that of tetracenes.[4i] By employing a donor−acceptor strategy to promote antiparallel π−π stacking, Swager and co-workers demonstrated that fluorine- and alkyl/alkoxy-functionalized tetracenes confine their solid-state packing to a slipped cofacial motif.[4j] Similarly, Nuckolls' group showed that the donor−acceptor interactions between dipolar acenes afforded antiparallel π−π stacking, and the mobility and I_{on}/I_{off} of its OFET device fabricated on an OTS-treated silicon oxide were 10^{-2} cm^2 s^{-1} V^{-1} and $\geq 10^{-6}$, respectively.[4k]

Due to our interest in crystal engineering and OFET materials, we set out to synthesize compounds that have the tendency to form a face-to-face π−π stacking structure. The strategies to obtaining face-to-face π−π stacked aromatic rings with tethers[7] or hydrogen bonds[8] often suffer from unfavorable π-electron repulsions and result in offset stacking of aromatic rings which decreases the effective overlap of the π orbitals. In contrast, an electron-rich aromatic ring and an electron-deficient perfluoro aromatic ring interact favorably and have a good tendency to form face-to-face π−π interaction.[9] In this study, we strategically construct bipolar molecules containing alternating electron-rich and electron-deficient moieties, aiming at favorable face-to-face π−π stacking for possible OFET applications. Structural determinations on two of the compounds were conducted by the single-crystal X-ray diffraction method. Theoretical carrier mobility based on the determined structures of the two compounds also will be described.

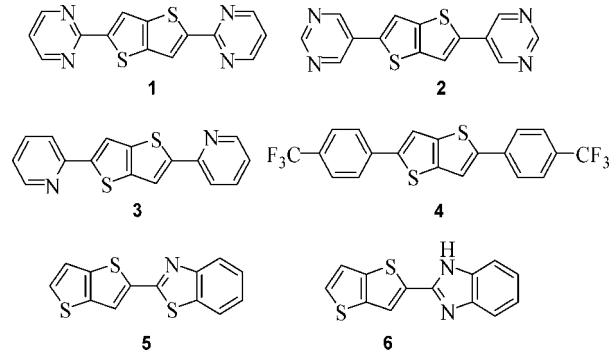

FIGURE 1. The structure of compounds **1**−**6**.

SCHEME 1

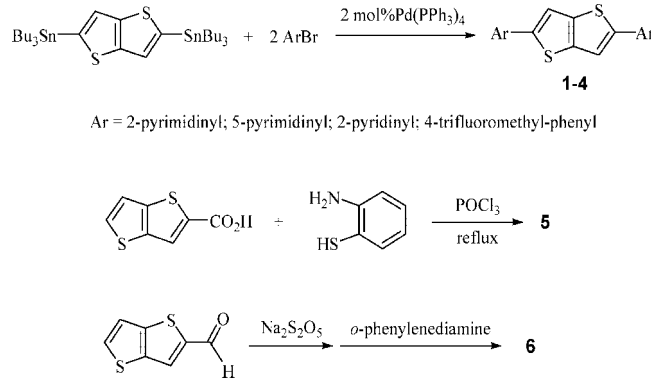

Results and Discussion

Synthesis and characterization. The new compounds synthesized are shown in Figure 1. They were obtained in moderate yields by the stepwise synthetic protocol illustrated in Scheme 1. Compounds **1**−**4** were synthesized via palladium(0)-catalyzed Stille coupling of 2,5-bis(tributylstannyl)thieno[3,2-*b*]thiophene with appropriate aryl bromides. The prototype synthesis of benzothiazole moiety was followed to prepare **5**:[10] condensation from thieno[3,2-*b*]thiophene-2-carboxylic acid and 2-aminothiophenol in the presence of $POCl_3$. Compound **6** was obtained from the condensation of *o*-phenylenediamine with the $Na_2S_2O_5$ adduct of thieno[3,2-*b*]thiophene-2-carbaldehyde.[11] Relevant spectral data are listed in Table 1. The vibronic feature observed in both the absorption and emission spectra implies the rigidity of the compounds. These compounds are highly crystalline, and the melting temperatures measured by DSC are 397, 329, 318, 340, 205, and 281 °C for **1**, **2**, **3**, **4**, **5**, and **6**, respectively.

Analysis of X-ray Crystal Structures and Theoretical Calculations. The structures of **2** and **5** (Figure 2) were also confirmed by the single-crystal X-ray diffraction method. There exists an inversion center passing through the midpoint of the C3−C3′ bond (ORTEP plot in Figure 2a) of the thieno[3,2-*b*]thiophene unit in **2**. The molecule is nearly coplanar with a small twist angle (7.4°) between the central thieno[3,2-*b*]thiophene ring and the peripheral pyrimidine ring. Compound

(4) (a) Anthony, J. E.; Brooks, J. S.; Eaton, D. L.; Parkin, S. R. *J. Am. Chem. Soc.* **2001**, *123*, 9482. (b) Anthony, J. E.; Eaton, D. L.; Parkin, S. R. *Org. Lett.* **2002**, *4*, 15. (c) Payne, M. M.; Parkin, S. R.; Anthony, J. E.; Kuo, C. C.; Jackson, T. N. *J. Am. Chem. Soc.* **2005**, *127*, 4986. (d) Park, S. K.; Jackson, T. N.; Anthony, J. E.; Mourey, D. A. *Appl. Phys. Lett.* **2007**, *91*, 063514. (e) Kobayashi, K.; Masu, H.; Shuto, A.; Yamaguchi, K. *Chem. Mater.* **2005**, *17*, 6666. (f) Sasaki, H.; Wakayama, Y.; Chikyow, T.; Barrena, E.; Dosch, H.; Kobayashi, K. *Appl. Phys. Lett.* **2006**, *88*, 081907. (g) Kobayashi, K.; Shimaoka, R.; Kawahata, M.; Yamanaka, M.; Yamaguichi, K. *Org. Lett.* **2006**, *8*, 2385. (h) Briseno, A. L.; Miao, Q.; Ling, M.-M.; Reese, C.; Meng, H.; Bao, Z.; Wudl, F. *J. Am. Chem. Soc.* **2006**, *128*, 15576. (i) Moon, H.; Zies, R.; Borkent, E. J.; Besnard, C.; Lovinger, A. J.; Siegrist, T.; Kloc, C.; Bao, Z. *J. Am. Chem. Soc.* **2004**, *126*, 15322. (j) Chen, Z.; Müller, P.; Swager, T. M. *Org. Lett.* **2006**, *8*, 273. (k) Miao, Q.; Lefenfeld, M.; Nguyen, T.-Q.; Siegrist, T.; Kloc, C.; Nuckolls, C. *Adv. Mater.* **2005**, *17*, 407.

(5) (a) Cornil, J.; Beljonne, D.; Calbert, J. P.; Brédas, J.-L. *Adv. Mater.* **2001**, *13*, 1053. (b) Cornil, J.; Calbert, J. P.; Brédas, J.-L. *J. Am. Chem. Soc.* **2001**, *123*, 1250. (c) Brédas, J.-L.; Cornil, J.; da, S.; Filho, D. A.; Cornil, J. *Proc. Natl. Acad. Sci. U.S.A.* **2002**, *99*, 5804. (d) Dimitrakopoulos, C. D.; Purushothaman, S.; Kymissis, J.; Callegari, A.; Shaw, J. M. *Science* **1999**, *283*, 822. (e) Dimitrakopoulos, C. D.; Kymissis, J.; Purushothaman, S.; Neumayer, D. A.; Duncombe, P. R.; Laibowitz, R. B. *Adv. Mater.* **1999**, *11*, 1372.

(6) (a) Bleiholder, C.; Werz, D. B.; Köppel, H.; Gleiter, R. *J. Am. Chem. Soc.* **2006**, *128*, 2666. (b) Gleiter, R.; Werz, D. B. *Chem. Lett.* **2005**, *34*, 126.

(7) Paraschir, I.; Giesbers, M.; van Lagen, B.; Grozema, F. C.; Siebbeles, L. D. A.; Marcelis, A. T. M.; Zuilhif, H.; Sudhölter, E. J. R. *Chem. Mater.* **2006**, *18*, 968.

(8) Lokey, R. S.; kwok, Y.; Guelev, V.; Pursell, C. J.; Hurley, L. H.; Iversen, B. L. *J. Am. Chem. Soc.* **1997**, *119*, 7202.

(9) Kim, T.-D.; Kang, J.-W.; Luo, J.; Jang, H.-S.; Ka, J.-W.; Tucker, N.; Benedict, J. B.; Dalton, L. R.; Gray, T.; Overney, R. M.; Park, D. H.; Herman, W. N.; Jen, A. K.-Y. *J. Am. Chem. Soc.* **2007**, *129*, 488. (b) Yoon, M.-H.; Facchetti, A.; Stern, C. E.; Marks, T. J. *J. Am. Chem. Soc.* **2006**, *128*, 5792.

(10) Wolfe, J. F.; Loo, B. H.; Arnold, F. E. *Macromolecules* **1981**, *14*, 915.

(11) (a) Goker, H.; Kus, C.; Boykin, D. W.; Yildiz, S.; Altanlar, N. *Bioorg. Med. Chem.* **2003**, *10*, 2589. (b) Ridley, H. F.; Spickett, R. G. W.; Timmis, G. M. *Heterocycl. Chem.* **1965**, *2*, 453.

(12) Valiyev, F.; Hu, W.-S.; Chen, H.-Y.; Kuo, M.-Y.; Chao, I.; Tao, Y.-T. *Chem. Mater.* **2007**, *19*, 3018.

(13) Siegrist, T.; Kloc, C.; Schön, J. H.; Batlogg, B.; Hadon, R. C.; Berg, S.; Thomas, G. A. *Angew. Chem., Int. Ed.* **2001**, *40*, 1732.

TABLE 1. Absorption and Emission Spectral Data of Thieno[3,2-*b*]thiophene Derivatives[a]

compd	λ_{max}, nm	λ_{em}, nm	Φ, %
1	340, 360, 390	395, 420	21
2	347	387, 415	43
3	361, 380	414, 425	41
4	357	396, 427	44
5	352, 370	391, 415	42
6	325, 340, 360	371, 388, 413	49

[a] The absorption and emission spectra were measured in CH_2Cl_2. The fluorescence quantum yield (Φ) was measured in CH_2Cl_2 relative to coumarin-1 (73%) in EtOH.

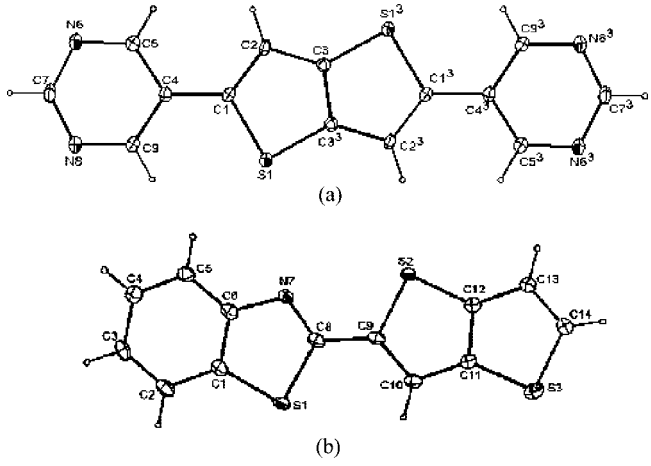

FIGURE 2. ORTEP plots of compounds **2** (a) and **5** (b).

5 is also nearly coplanar, and the twist angle between the thieno[3,2-*b*]thiophene ring and the benzothiazole ring is only 2.7°. The packing of the molecules inside the crystal lattice of **2** and **5** viewing along the long and short axes of the molecule is illustrated in Figure 3. For **2**, no herringbone structure is observed and the arrangement of the molecules can be basically described as a one-dimensional slipped-stack, with the interfacial distance of adjacent molecules being 3.47 Å (see *d* in Figure 3). In **5**, the edge-to-face interactions occur only at the terminal rings (i.e., at the short edges of the molecule, in direct contrast to pentacene and perfluoropentacene where the edge-to-face interactions occur along the long molecular edges). Nevertheless, the $\pi-\pi$ interfacial distance of the adjacent molecules is 3.59 Å within the same stack (Figure 3). Both crystals **2** and **5** therefore have favorable $\pi-\pi$ interaction to facilitate charge-carrier hopping among molecules in the direction perpendicular to the molecular plane. It is also noted that $\pi-\pi$ interaction exists between the electron-rich moiety of each molecule and the electron-deficient moiety of the next stacked molecule. The thieno[3,2-*b*]thiophene (electron rich) unit is right above half of the pyrimidine (electron deficient) unit for **2**, with a short on-top intrastack S···C contact of 3.34 Å, and thieno[3,2-*b*]thiophene is above part of the benzothiazole moiety for **5**. No S···S contact has been found in either crystal, but the N···S interstack contact (3.27 Å) has been found for **5**.

Curtis et al. have analyzed the spatial relationship of molecules in the crystal structures of substituted pentacenes, bithiazole- and thiophene-containing oligomers with "pitch" (*P*) and "roll" (*R*) angles.[3] Briefly, the smaller the angles $\angle P$ or $\angle R$, the smaller the slip distances along the long (d_p: the pitch distance) or short axis (d_r: the roll distance) (Figure 3). One of the key criteria for good $\pi-\pi$ stacking is the molecular width (w) to d_r ratio (w/d_r); for good $\pi-\pi$ stacking, $w/d_r \geq 1$ is required, and the importance of small d_r has been stressed.[3] Roll distances larger than ca. 2.8 Å can seriously damage the $\pi-\pi$ overlap between nearest-neighboring molecules because the widths of the organic materials Curtis et al. investigated are within the range of 2.8 Å (the approximate width of benzene).

Table 2 shows the results of the same phenomenological analysis for pentacene, **2**, and **5**. The d_p of **2** (2.78 Å) is similar to that of the pentacene dimer (2.10 Å), while large slip along the long axis is observed for **5** (4.85 Å). Along the molecular short axis, an extremely small d_r of only 0.06 Å is observed for **2**; for **5**, a d_r of 0.55 Å also reveals a small short-axial slip. So far, a d_r of 0.06 Å is the smallest slip distance found including those data obtained in Curtis' study.[3] Negligible slip along the short axis and moderate slip along the long axis could be two of the factors that explains why **2** has a significant calculated electronic coupling value of 0.153 eV (t^+ in Table 3), which is twice as large as that of the largest coupling of pentacene. As the rate of charge transfer is proportional to the square of t in Marcus theory, the rate of hole transport of **2** could be four times that of pentacene, assuming factors other than t are kept the same.

It can be seen from Table 3 that t^+ values of **2** and **5** are appreciably larger than their respective t^- values. This trend can be understood qualitatively according to the shapes of the frontier orbitals. Good orbital overlaps between the frontier orbitals of interacting molecules result in large t values. When an orbital (e.g., a p orbital) is above the nodal plane of the molecular orbital of another molecule (e.g., the π^* orbital of ethylene), the positive and negative overlaps between molecules cancel out and afford negligible electronic coupling. For LUMOs of **2** and **5** (related to t^-), nodal planes are found parallel to both the long and short molecular axes, while nodal planes are only found along the short molecular axes for HOMOs (related to t^+). (See Figure 4.) Therefore, when the slip distances are nonzero, it is of higher probability for **2** and **5** to have large t^+ values than to have large t^- values (due to fewer nodal planes in HOMO than in LUMO). This argument has been introduced by Troisi to explain results of cofacially stacked pentacene systems.[14] Nevertheless, the situation is reversed in the cases of pentacene derivatives: nodal planes are found along both the short and long molecular axes for the HOMOs, but this is not the case for the LUMOs. Finally, it is noted that the donor and acceptor parts of **2** and **5** do not result in localized frontier orbitals; both the HOMOs and LUMOs spread out over the entire molecule, rather than localize at small regions. MOs localized in small regions are likely to afford ineffective electronic couplings. Therefore, the introduction of polar groups in **2** and **5** does not seem to have a negative effect on *t*.

The nearly on-top intrastack S···C contacts observed in **2** warrant further discussions in terms of crystal engineering and electronic coupling. For each dimer of **2**, the relative spatial disposition is stapled by a pair of symmetrical S···C contacts (Figure 5a), so that d_r is nearly zero and d_p is moderate. The interaction between the electron-rich S atom and the electron-deficient C atom has to be quite favorable, as the pyrimidine plane becomes slightly out-of-plane with respect to the central thieno[3,2-*b*]thiophene unit. Considering the larger van der Waals radius of an S atom than that of a C atom, the S···C contact (3.34 Å) is *significantly* shorter than the nearby C···C distance (3.63 Å) (Figure 5a). In terms of crystal engineering, the above results imply the possibility to deem the nonbonded

(14) Troisi, A.; Orlando, G.; Anthony, J. E. *Chem. Mater.* **2005**, *17*, 5024.

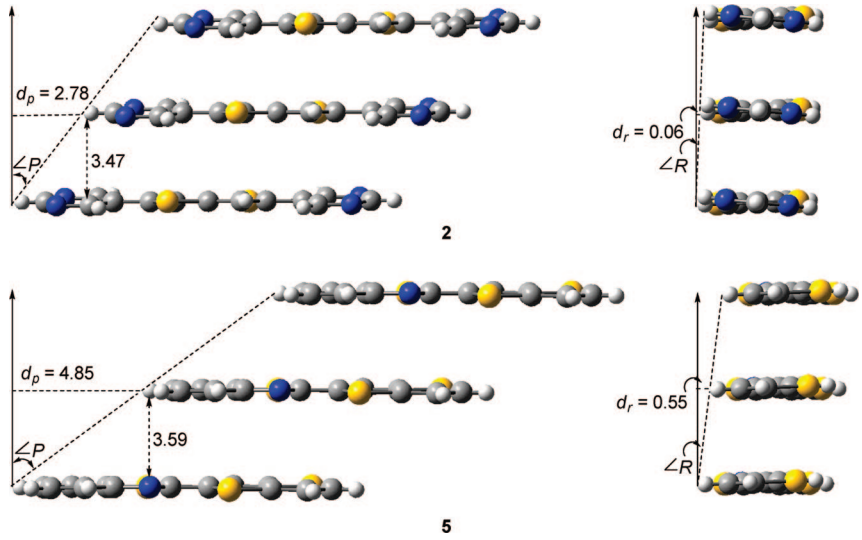

FIGURE 3. Schematic illustrations of "pitch" and "roll" angles/distances ($\angle P/d_p$; $\angle R/d_r$) for **2** and **5** as defined by Curtis et al.[3] The interfacial distances (d) are also given. Distances are in Å.

TABLE 2. Structural Characterization of Pentacene, 2, and 5 with Pitch (*P*) and Roll (*R*) Angles and Distances

compd	*P* (deg)	*R* (deg)	*d* (Å)	d_p (Å)	d_r (Å)	*z* (Å)[a]
pentacene[b]	39.1	64.2	2.58	2.10	5.35	6.30
2	38.7	1.0	3.47	2.78	0.06	4.44
5	53.5	8.8	3.59	4.85	0.55	6.06

[a] $z = (d_p^2 + d_r^2 + d^2)^{1/2}$. The deviations of *z* values from the crystallographic stacking distances (i.e., the distance between two identical parts of two adjacent molecules) are 0.4%, 0.0%, and 0.4% for pentacene, **2**, and **5**, respectively. These small values ensure the quality of estimated pitch/roll angles and distances measured with the program Mercury. [b] Data taken from ref 3.

relationship between the electron-deficient pyrimidine and the electron-rich thieno[3,2-*b*]thiophene a synthon for face-to-face π-stacking. So far, no other crystal structure with the coexistence of the pyrimidine and thieno[3,2-*b*]thiophene moieties can be found in the Cambridge Structure Database. Therefore, systematic studies are needed to investigate whether the above two units can really be regarded as a synthon for face-to-face stacking. In Figure 5b, the HOMO-1 of dimers of **2** are shown (HOMO-1 of the dimer is the positive coupling between HOMOs of the monomer). It is clear that the nearly *on-top* S···C contacts facilitate good coupling between monomers.

At room temperature, the hopping mechanism for the charge-transport process is believed to be important for thin-film OFET.[5a,b,15] Under this mechanism, the rate of charge-transport is described by Marcus theory,[16] in which both *t* and reorganization energy, λ, are important factors. The calculated internal reorganization energies ($\lambda^{\pm}$) of **2** and **5** are shown in Table 3. Results of **2** for the fully optimized and the partially constrained quasiplanar geometries (the two terminal inter-ring dihedral angles were constrained to the value found in the crystal structure) are both shown in the Table 3. Since the quasiplanar geometry of **2** may better reflect the molecular structure in the packing of an OFET device, we use the latter data in the following discussion.

The significantly larger $\lambda^{\pm}$ values (>0.26 eV) of **2** and **5** compared to that of pentacene (<0.14 eV) show the price one has to pay for employing thieno[3,2-*b*]thiophene, benzothiazole, and pyrimidine as charge-transport units. The large $\lambda^{\pm}$ values (Table 3) for **2** and **5** can be associated with the large bond length alterations (BLAltr) between the neutral and charged states. For pentacene, the BLAltr are in the range of 0.004−0.016 Å upon oxidation and reduction.[17] Whereas, the BLAltr of **2** for hole- and electron-transfer processes are in the range of 0.001−0.034 and 0.005−0.034 Å, respectively; and those of **5** are 0.001−0.034 and 0.003−0.046 Å, respectively. Notably, significant BLAltr are observed for the *inter-ring* distances in both **2** and **5**, in accord with the orbital distributions across the inter-ring regions (Figure 4). In the anionic state, the *inter-ring* BLAltr (0.034 Å for **2**, and 0.046 Å for **5**) are the largest among all BLAltr.

It has been shown in the literature that reasonable qualitative estimates of charge mobilities ($\mu^{\pm}$) can be calculated with λ, *t*, and experimentally determined intermolecular distance (see computational details).[12,18] Despite of the inferior $\lambda^{\pm}$ values compared to those of pentacene, the impressive t^{+} value of **2** still renders good theoretical hole mobility (μ^{+}, 2.32 $cm^2\ s^{-1}\ V^{-1}$). The μ^{+} of **5** (0.60 $cm^2\ s^{-1}\ V^{-1}$) and μ^{-} (0.18 $cm^2\ s^{-1}\ V^{-1}$) of **2** are an order of magnitude smaller, and the μ^{-} of **5** is the smallest due to an even smaller t^{-} and a large λ^{-}. As pentacene is basically a *p*-channel OFET material in a normal device configuration, it is of interest to learn the effect the heteroaromatic units in **2** and **5** in terms of polarity of the semiconductors. According to the calculated electron affinities (EA), the smaller EA values of **2** and **5** compared to that of pentacene (Table 3) prevent them from being *n*-channel materi-

(15) (a) Mas-Torrent, M.; Hadley, P.; Bromley, S. T.; Ribas, X.; Tarrés, J.; Mas, M.; Molins, E.; Veciana, J.; Rovira, C. *J. Am. Chem. Soc.* **2004**, *126*, 8546. (b) Bromley, S. T.; Mas-Torrent, M.; Hadley, P.; Rovira, C. *J. Am. Chem. Soc.* **2004**, *126*, 6544. (c) da Silva Filho, D.; Olivier, Y.; Coropceanu, V.; Brédas, J.-L.; Cornil, J. Theoretical Aspects of Charge Transport. In *Organic Semiconductors: A Molecular Perspective. In Organic Field-Effect Transistors*; Bao, Z., Locklin, J., Eds.; CRC: Boca Raton, FL, 2007; Chapter 1.

(16) (a) Marcus, R. A. *Annu. Rev. Phys. Chem.* **1964**, *15*, 155. (b) Marcus, R. A.; Sutin, N. *Biochem. Biophys. Acta* **1985**, *811*, 265. (c) Newton, M. D.; Sutin, N. *Annu. Rev. Phys. Chem.* **1984**, *35*, 437. (d) Barbara, P. F.; Meyer, T. J.; Ratner, M. A. *J. Phys. Chem.* **1996**, *100*, 13148.

(17) Chen, H. Y.; Chao, I. *Chem. Phys. Lett.* **2005**, *401*, 539.

(18) (a) Lemaur, V.; da Silva Filho, D. A.; Coropceanu, V.; Lehmann, M.; Geerts, Y.; Piris, J.; Debije, M. G.; van de Graats, A. M.; Senthilkumar, K.; Siebbeles, L. D. A.; Warman, J. M.; Brédas, J.-L.; Cornil, J. *J. Am. Chem. Soc.* **2004**, *126*, 3271. (b) CornilJ, J.; Lemaur, V.; Calbert, J. P.; Brédas, J.-L. *Adv. Mater.* **2002**, *14*, 726. (c) Song, Y.; Di, C.; Yang, X.; Li, S.; Xu, W.; Liu, Y.; Yang, L.; Shuai, Z.; Zhang, D.; Zhu, D. *J. Am. Chem. Soc.* **2006**, *128*, 15940. (d) Kuo, M.-Y.; Chen, H.-Y.; Chao, I. *Chem. Eur. J.* **2007**, *13*, 4750.

TABLE 3. Calculated Adiabatic Ionization Potentials (IP) and Electron Affinities (EA), Reorganization Energies of the Charge Transport ($\lambda^{\pm}$), Electronic Couplings ($t^{\pm}$), and Mobilities ($\mu^{\pm}$)

compd	$d_{c\text{-}c}$[d] (Å)	IP (eV)	λ^+ (eV)	t^+ (eV)	μ^+ (cm^2 s^{-1} V^{-1})	EA (eV)	λ^- (eV)	t^- (eV)	μ^- (cm^2 s^{-1} V^{-1})
pentacene[a]	6.27	5.899	0.094	0.034	1.93	1.136	0.133	0.046	2.03
	5.22			0.044	2.25			0.076	3.84
	4.76			0.075	5.43			0.078	3.35
2[b]	4.44	7.287	0.262	0.153	2.32	1.138	0.274	0.046	0.18
2[c]		7.310	0.309			1.121	0.419		
5	6.03	7.007	0.300	0.071	0.60	0.620	0.335	0.013	0.01

[a] Most data were taken from ref 12. The IP value of pentacene in ref 12 was incorrectly typed as 5.888 eV. Three distinct dimeric pairs were observed in the crystal structure of pentacene, and three sets of values were estimated for $t^{\pm}$ and $\mu^{\pm}$. The structure of pentacene was taken from ref 13. [b] Two inter-ring dihedral angels were frozen at the angles observed in the crystal structure. [c] Calculated based on the gas-phase optimized geometry. [d] Molecular center-to-center distance used in the estimation of charge mobility.

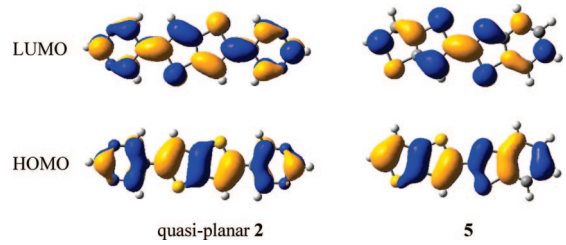

FIGURE 4. Frontier orbitals of **2** and **5**.

als in a regular OFET configuration, even though the electron-deficient moieties are present. On the other hand, the presence of electron-deficient moieties and the lack of extended conjugation have caused the ionization potentials (IP) to be quite large, which may impart higher oxidative stability for **2** and **5** compared to that of pentacene, but also result in higher hole injection barriers and higher sensitivity of the charge carriers to the traps caused by impurities.

Conclusion

Face-to-face π-stacked structure in the crystal lattice has been achieved with bipolar molecules containing alternate electron-rich thieno[3,2-*b*]thiophene units and electron-deficient pyrimidine or benzothiazole units. Owing to the favorable interactions between the thieno[3,2-*b*]thiophene and pyrimidine units (which is characterized by the symmetrical on-top S···C contacts), the nearly zero slip distance along the short molecular axis and the moderate slip distance along the long molecular axis in **2** result in a significant electronic coupling twice as large as that of pentacene for hole hopping. Good hole mobilities (μ^+) for **2** and **5** of 2.32 and 0.60 cm^2 s^{-1} V^{-1}, respectively, are predicted from the acceptable λ^+ (reorganization energy) and high t^+ (intermolecular electronic coupling). Overall, the attempt at coupling electron-rich and electron-deficient heteroaromatics is successful in terms of crystal engineering and electronic coupling. A new π-stacking synthon in crystal engineering has been proposed and will be examined further in the future. The theoretical analyses on internal reorganization energy, EA, and IP reveal the disadvantage of using small heteroaromatic rings. More extended rings will be considered in the future so that the reorganization energy can be lowered and the EA and IP can be tuned.

Experimental Methods

2,5-Di(pyrimidin-2-yl)thieno[3,2-*b*]thiophene (1). A two-necked round-bottomed flask was charged with 2-bromo-pyrimidine (1.11 g, 7.0 mmol), 2,5-bis(tributylstannyl)thieno[3,2-*b*]thiophene (2.37 g, 3.3 mmol), and $Pd(PPh_3)_4$ (2 mmol %, 76 mg). Dry DMF (10 mL) was added, and the mixture was heated at 80 °C under nitrogen for 24 h. After cooling, the solution was filtered, and the pale yellow precipitates collected were washed with acetone and EtOH several times. Crude product was further sublimed to afford pure **1** as bright yellow powders in 25% yield. ^{1}H NMR (δ, DMSO-d_6): 7.42 (t, 2 H, J = 4.7 Hz, pyrimidine), 8.36 (s, 2 H, thiophene), 8.86 (d, 4 H, J = 4.7 Hz, pyrimidine). The compound is not soluble enough for recording ^{13}C NMR soectra. EI MS (*m*/*z*): 296.0 [M$^+$]. HRMS (*m*/*z*): calcd for $C_{14}H_8N_4S_2$ 296.0190, found 296.0193 [M$^+$]. Anal. Calcd for $C_{14}H_8N_4S_2$: C, 56.74; H, 2.72; N, 18.90. Found: C, 56.79; H, 2.61; N, 18.86.

2,5-Di(pyrimidin-5-yl)thieno[3,2-*b*]thiophene (2). Essentially the same procedures as for the synthesis of **1** were used except that 5-bromopyrimidine was used instead of 2-bromopyrimidine. A bright yellow solid was obtained in 20% yield. ^{1}H NMR (δ, DMSO-d_6): 8.23 (s, 2 H, thiophene), 9.16 (s, 2 H, pyrimidine), 9.29 (s, 4 H, pyrimidine). ^{13}C NMR (δ, DMSO-d_6): 163.1, 157.4, 153.2, 138.6, 128.2, 119.1. FAB MS (*m*/*z*): 297.1 [M$^+$ + H]. HRMS (*m*/*z*): calcd for $C_{14}H_9N_4S_2$ 297.0269, found 297.0271 [M$^+$ + H]. Anal. Calcd for $C_{14}H_8N_4S_2$: C, 56.74; H, 2.72; N, 18.90. Found: C, 56.98; H, 2.74; N, 18.83.

2,5-Di(pyridin-5-yl)thieno[3,2-*b*]thiophene (3). Essentially the same procedures as for the synthesis of **1** were used except that 2-bromopyridine was used instead of 2-bromopyrimidine. After cooling, the reaction mixture was extracted with a mixture of saturated KF aqueous solution and CH_2Cl_2. The organic extracts were collected and dried over $MgSO_4$. The solution was then purified by column chromatography to provide **3** as a pale yellow powder in 25% yield. ^{1}H NMR (δ, $CDCl_3$): 7.16 (dd, 2 H, J = 8.7, 4.8 Hz, 2 H, pyridine), 7.69 (m, 4 H, pyrimidine), 7.77 (s, 2 H, thiophene), 8.57 (d, 2 H, J = 4.8 Hz, pyrimidine). ^{13}C NMR (δ, $CDCl_3$): 152.1, 149.5, 141.6, 136.9, 122.3, 119.0, 117.7. FAB MS (*m*/*z*): 295.2 [M$^+$ + H]. HRMS (*m*/*z*): calcd for $C_{16}H_{11}N_2S_2$ 295.0364, found 295.0366 [M$^+$ + H]. Anal. Calcd for $C_{16}H_{10}N_2S_2$: C, 65.28; H, 3.42; N, 9.52. Found: C, 65.01; H, 3.32; N, 9.34.

2,5-Bis(4-(trifluoromethyl)phenyl)thieno[3,2-*b*]thiophene (4). Essentially the same procedures as for the synthesis of **3** were used except that 1-bromo-4-(trifluoromethyl)benzene was used instead of 2-bromopyridine. A pale yellow solid was obtained in 20% yield. ^{1}H NMR (δ, $CDCl_3$): 7.57 (s, 2 H, thiophene), 7.65 (d, 4 H, J = 8.3 Hz, C_6H_4), 7.73 (d, 4 H, J = 8.3 Hz, C_6H_4). ^{13}C NMR (δ, $CDCl_3$): 126.1, 125.9, 125.8, 116.8, 115.0. FAB MS (*m*/*z*): 428.0 [M$^+$]. HRMS (*m*/*z*): calcd for $C_{20}H_{10}F_6S_2$ 428.0128, found 428.0129 [M$^+$]. Anal. Calcd for $C_{20}H_{10}F_6S_2$: C, 56.07; H, 2.35. Found: C, 56.09; H, 2.11.

2-Thieno[3,2-*b*]thiophene-2-yl-benzothiazole (5). A two-necked round-bottomed flask was charged with thieno[3,2-*b*]thiophene-2-carboxylic acid (3.0 g, 16 mmol), 2-aminothiophenol (2.25 g,, 1.92 mL, 18 mmol), and $POCl_3$ (20 mL). The mixture was refluxed for 12 h. After cooling, iced water was added, and the solution was neutralized by adding aqueous NaOH. The solution was extracted with CH_2Cl_2. The organic extracts were collected and dried over $MgSO_4$. The solution was further purified by column chromatography to provide **5** as a light brown powder in 11% (0.50 g) yield.

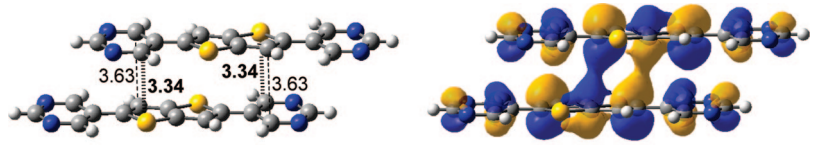

(a) (b)

FIGURE 5. (a) A pair of on-top S···C contacts (Å) can be found in the dimer of **2** (crystal structure). The nearby C···C distances are also labeled. (b) HOMO-1 of the dimer of **2** shows that the on-top contacts facilitate a good coupling between the HOMOs of the monomers.

^{1}H NMR (δ, acetone-d_6): 7.45 (td, 1 H, J = 7.2, 1.2 Hz, C_6H_4), 7.51 (d, 1 H, J = 5.2 Hz, thiophene), 7.55 (td, 1 H, J = 7.2, 1.2 Hz, C_6H_4), 7.80 (d, 1 H, J = 5.2 Hz, thiophene), 7.99 (d, 1 H, J = 8.0 Hz, C_6H_4), 8.07 (d, 1 H, J = 8.0 Hz, C_6H_4), 8.14 (s, 1 H, thiophene). ^{13}C NMR (δ, acetone-d_6): 163.7, 154.7, 145.0, 139.9, 136.4, 133.3, 132.0, 127.6, 127.0, 126.5, 123.7, 122.9, 122.6, 121.0. FAB MS (*m*/*z*): 274.1 [M^+ + H]. HRMS (*m*/*z*): calcd for $C_{13}H_8NS_3$ 273.9819, found 273.9818 [M^+ + H]. Anal. Calcd for $C_{13}H_7NS_3$: C, 57.11; H, 2.58; N, 5.12. Found: C, 56.37; H, 2.13; N, 5.30.

2-Thieno[3,2-*b*]thiophene-2-yl-1*H*-benzoimidazole (6). To a flask containing thieno[3,2-*b*]thiophene (1.4 g, 10 mmol) in 40 mL of DMF immersed in a cold bath at 0 °C was added *n*-BuLi (7.0 mL, 1.6 M in hexane) dropwise. After addition was complete, the solution was stirred for 1 h. Another 10 mL of DMF was added and the solution was stirred for an additional 20 min at 0 °C. After the solution was warmed to room temperature, the solution was extracted with Et_2O. The ether extracts were collected and dried over $MgSO_4$. The solvent was removed in vacuo to provide yellow oily thieno[3,2-*b*]thiophene-2-carbaldehyde. To a flask containing thieno[3,2-*b*]thiophene-2-carbaldehyde (1.51 g, 9.0 mmol) in 30 mL of EtOH immersed in a cold bath at 0 °C was added dropwise 30 mL of aqueous solution containing $Na_2S_2O_5$ (10.8 mmol). The solution was stirred at 0 °C for 6 h and filtered. The yellow hydroxylthieno[3,2-*b*]thiophene-2-ylmethanesulfonate collected was washed with H_2O and EtOH and pumped dry. A flask was charged with hydroxylthieno[3,2-*b*]thiophene-2-ylmethanesulfonate and 17 mL of DMF. After being stirred at 130 °C, the solution was cooled to room temperature. The solid formed upon addition of H_2O was collected by filtration. It was then extracted with a mixture of CH_2Cl_2 and saturated brine. The organic extracts were collected and dried over $MgSO_4$. After removal of the solvent, the residue was recrystallized from CH_2Cl_2/hexane to afford off-white **6** in 15% yield. ^{1}H NMR (δ, acetone-d_6): 7.19−7.23 (m, 2 H, C_6H_4), 7.48 (d, 1 H, J = 5.2 Hz, thiophene), 7.48−7.51 (m, 1 H, C_6H_4), 7.63−7.67 (m, 1 H, C_6H_4), 7.71 (d, 1 H, J = 5.2 Hz, thiophene), 8.08 (s, 1 H, thiophene). ^{13}C NMR (δ, acetone-d_6): 148.3, 145.3, 141.8, 140.6, 136.9, 136.0, 130.5, 124.0, 123.0, 120.9, 120.0, 119.4, 111.9. FAB MS (*m*/*z*): 257.1 [M^+ + H]. HRMS (*m*/*z*): calcd for $C_{13}H_9N_2S_2$ 257.0207, found 257.0202 [M^+ + H]. Anal. Calcd for $C_{13}H_8N_2S_2$: C, 60.91; H, 3.15; N, 10.93. Found: C, 61.26; H, 3.16; N, 10.96.

(19) Frisch, M. J.; Trucks, G. W.; Schlegel, H. B.; Scuseria, G. E.; Robb, M. A.; Cheeseman, J. R.; Montgomery, J. A., Jr.; Vreven, T.; Kudin, K. N.; Burant, J. C.; Millam, J. M.; Iyengar, S. S.; Tomasi, J.; Barone, V.; Mennucci, B.; Cossi, M.; Scalmani, G.; Rega, N.; Petersson, G. A.; Nakatsuji, H.; Hada, M.; Ehara, M.; Toyota, K.; Fukuda, R.; Hasegawa, J.; Ishida, M.; Nakajima, T.; Honda, Y.; Kitao, O.; Nakai, H.; Klene, M.; Li, X.; Knox, J. E.; Hratchian, H. P.; Cross, J. B.; Bakken, V.; Adamo, C.; Jaramillo, J.; Gomperts, R.; Stratmann, R. E.; Yazyev, O.; Austin, A. J.; Cammi, R.; Pomelli, C.; Ochterski, J. W.; Ayala, P. Y.; Morokuma, K.; Voth, G. A.; Salvador, P.; Dannenberg, J. J.; Zakrzewski, V. G.; Dapprich, S.; Daniels, A. D.; Strain, M. C.; Farkas, O. ; Malick, D. K.; Rabuck, A. D.; Raghavachari, K.; Foresman, J. B.; Ortiz, J. V.; Cui, Q.; Baboul, A. G.; Clifford, S.; Cioslowski, J.; Stefanov, B. B.; Liu, G.; Liashenko, A.; Piskorz, P.; Komaromi, I.; Martin, R. L.; Fox, D. J.; Keith, T.; Al-Laham, M. A.; Peng, C. Y.; Nanayakkara, A.; Challacombe, M.; Gill, P. M. W.; Johnson, B.; Chen, W.; Wong, M. W.; Gonzalez, C.; Pople, J. A. *Gaussian 03*, Revision D.02; Gaussian, Inc.: Wallingford, CT, 2004.

(20) (a) Coropceanu, V.; Malagoli, M.; da Silva Filho, D. A.; Gruhn, N. E.; Bill, T. G.; Brédas, J. L. *Phys. Rev. Lett.* **2002**, *89*, 275503. (b) Kwon, O.; Coropceanu, V.; Gruhn, N. E.; Durivage, J. C.; Laquindanum, J. G.; Katz, H. E.; Cornil, J.; Brédas, J. L. *J. Chem. Phys.* **2004**, *120*, 8186. (c) Chen, H. Y.; Chao, I. *ChemPhysChem* **2006**, *7*, 2003.

Computational Methods

All the structures were optimized at the DFT-B3LYP/6-31G(d,p) level of theory and frequency calculations were performed to confirm whether the optimized geometry was an energy minimum on the potential energy surface with Gaussian 03.[19] ($\langle S^2 \rangle$ for the open-shell species is in the range of 0.7615−0.7702.) At high temperature (including room temperature), the charge carriers in thin-film OFET are believed to be localized at individual molecules, and the charge-transport mechanism is a hopping mechanism described by Marcus theory.[16] The rate expression of self-exchange process is:

$$k_{et} = \frac{4\pi^2}{h}\frac{1}{\sqrt{4\pi\lambda k_B T}} t^2 \exp(-\frac{\lambda}{4k_B T}) \quad (1)$$

in which the internal reorganization energy (λ) and intermolecular electronic coupling (t) decide the value of the electron transfer rate (k_{et}).

Because the reorganization energies (λ) calculated at the DFT-B3LYP/6-31G(d,p) level agree well with experimental values,[15b,17,20] λ is estimated at the same theory level. The total internal reorganization energy ($\lambda^{\pm}$) is the sum of $\lambda_1^{\pm}$ and $\lambda_2^{\pm}$ (see eqs 2−4):

$$\lambda^{\pm} = \lambda_1^{\pm} + \lambda_2^{\pm} \quad (2)$$

$$\lambda_1 = E_{\pm}(Q_N) - E_{\pm}(Q_{\pm}) \quad (3)$$

$$\lambda_2 = E_N(Q_{\pm}) - E_N(Q_N) \quad (4)$$

where $E_{\pm}(Q_N)$ is the total energy of the charged state in the neutral geometry, $E_{\pm}(Q_{\pm})$ is the total energy of the charged state in the charged state geometry, $E_N(Q_{\pm})$ is the total energy of the neutral state in the charged state geometry, and $E_N(Q_N)$ is the total energy of the neutral state in the neutral geometry.

The $t^{\pm}$ values were obtained via the direct coupling method (eq 5) with the use of dimeric structures extracted from the X-ray structures. The fragmental orbital approach implemented in the Amsterdam density functional (ADF) program[21] was used to derive the components in eq 5. The details are described in two recent papers.[22] The DZP basis set in ADF was used and the local density functional VWN was employed in conjunction with the PW91 gradient corrections.

$$t^{\pm} = \frac{H_{RP} - S_{RP}(H_{RR} + H_{PP})/2}{1 - S_{RP}^2} \quad (5)$$

where H_{RP} is the charge transfer integrals, S_{RP} is the spatial overlap, and H_{RR} and H_{PP} are site energies.

Once $\lambda^{\pm}$ and $t^{\pm}$ are obtained, one can calculate the electron transfer rate k_{et} according to eq 1. The diffusion coefficient D of charge carriers can then be given by eq 6, where L is the effective

(21) (a) te Velde, G.; Bickelhaupt, F. M.; van Gisbergen, S. J. A.; Guerra, C. F.; Baerends, E. J.; Snijders, J. G.; Ziegler, T. *J. Comput. Chem.* **2001**, *22*, 931. (b) Fonseca Guerra, C.; Snijders, J. G.; te Velde, G.; Baerends, E. J. *Theor. Chem. Acc.* **1998**, *99*, 391. (c) ADF 2005 01, SCM, Theoretical Chemistry, Vrije Universiteit: Amsterdam, The Netherlands, http://www.scm.com.

(22) (a) Prins, P.; Senthilkumar, K.; Grozema, F. C.; Jonkheijm, P.; Schenning, A. P. H. J.; Meijer, E. W.; Siebbeles, L. D. A. *J. Phys. Chem. B* **2005**, *109*, 18267. (b) Senthilkumar, K.; Grozema, F. C.; Buckelhaupt, F. M.; Siebbeles, L. D. A. *J. Chem. Phys.* **2003**, *119*, 9809.

length of electron transfer (L was approximated by the molecular center-to-center distance of a dimer). This allows us to evaluate the drift mobility of charge from the Einstein relation,[23] as shown in eq 7, where e is the electronic charge, k_B is Boltzmann constant,

$$D = L^2 k_{et}/2 \quad (6)$$

$$\mu = eD/k_B T \quad (7)$$

and T is temperature in Kelvin (300 K in this study). This method has been employed for the calculation of the charge carrier mobility of organic seimconductors.[12,18]

(23) Atkins, P. W. *Physical Chemistry*, 4th ed.; Oxford University Press: Oxford, UK, 1990.

Acknowledgement. We thank the National Science Council and Academia Sinica for the financial support. The computing time granted by the National Center for High-Performance Computing and the Computing Center of Academia Sinica is also acknowledged.

Supporting Information Available: Complete crystallographic data and calculated coordinates of compounds **2** and **5** and copies of ^{1}H and ^{13}C spectra for the new compounds. This material is available free of charge via the Internet at http://pubs.acs.org.

JO800546J